Environmental Science & Technology

Article

pubs.acs.org/est

Iron-Mediated Anaerobic Oxidation of Methane in Brackish Coastal Sediments

Matthias Egger,*[,†] Olivia Rasigraf,[‡] Célia J. Sapart,[§,∥] Tom Jilbert,[†,⊥] Mike S. M. Jetten,[‡] Thomas Röckmann,[§] Carina van der Veen,[§] Narcisa Bândă,[§] Boran Kartal,[‡,#] Katharina F. Ettwig,[‡] and Caroline P. Slomp[†]

[†]Department of Earth Sciences - Geochemistry, Faculty of Geosciences, Utrecht University, Budapestlaan 4, 3584 CD Utrecht, The Netherlands

[‡]Department of Microbiology, Institute for Water and Wetland Research, Faculty of Science, Radboud University Nijmegen, Heyendaalseweg 135, 6525 AJ Nijmegen, The Netherlands

[§]Institute for Marine and Atmospheric Research Utrecht (IMAU), Utrecht University, Princetonplein 5, 3584 CC Utrecht, The Netherlands

[∥]Laboratoire de Glaciologie, Université Libre de Bruxelles, 50 Avenue F. D. Roosevelt, B-1050 Bruxelles, Belgium

[#]Department of Biochemistry and Microbiology, Laboratory of Microbiology, Ghent University, K. L. Ledeganckstraat 35, 9000 Gent, Belgium

Supporting Information

ABSTRACT: Methane is a powerful greenhouse gas and its biological conversion in marine sediments, largely controlled by anaerobic oxidation of methane (AOM), is a crucial part of the global carbon cycle. However, little is known about the role of iron oxides as an oxidant for AOM. Here we provide the first field evidence for iron-dependent AOM in brackish coastal surface sediments and show that methane produced in Bothnian Sea sediments is oxidized in distinct zones of iron- and sulfate-dependent AOM. At our study site, anthropogenic eutrophication over recent decades has led to an upward migration of the sulfate/methane transition zone in the sediment. Abundant iron oxides and high dissolved ferrous iron indicate iron reduction in the methanogenic sediments below the newly established sulfate/methane transition. Laboratory incubation studies of these sediments strongly suggest that the in situ microbial community is capable of linking methane oxidation to iron oxide reduction. Eutrophication of coastal environments may therefore create geochemical conditions favorable for iron-mediated AOM and thus increase the relevance of iron-dependent methane oxidation in the future. Besides its role in mitigating methane emissions, iron-dependent AOM strongly impacts sedimentary iron cycling and related biogeochemical processes through the reduction of large quantities of iron oxides.

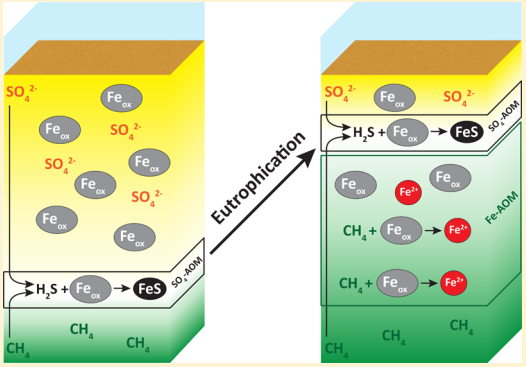

INTRODUCTION

Methane (CH_4) is a potent greenhouse gas in the Earth's atmosphere with a global warming potential 28−34 times that of carbon dioxide (CO_2) on a centennial time scale.[1] Anaerobic oxidation of methane (AOM) efficiently controls the atmospheric CH_4 efflux from the ocean by consuming an estimated >90% of all the CH_4 produced in marine sediments.[2,3] Most of this AOM is attributed to sulfate (SO_4^{2-}) reduction[4−10] (SO_4-AOM, eq 1), but oxidized solid phases such as iron (Fe)-oxides are also thermodynamically favorable electron acceptors for the biological oxidation of CH_4 (eq 2).

$$CH_4 + SO_4^{2-} \rightarrow HS^- + HCO_3^- + H_2O \quad (1)$$

$$CH_4 + 8Fe(OH)_3 + 15H^+ \rightarrow HCO_3^- + 8Fe^{2+} + 21H_2O \quad (2)$$

The co-occurrence of reactive Fe-oxides and CH_4 in freshwater[11−14] and some brackish[15,16] sedimentary environments suggests that AOM coupled to Fe-oxide reduction (Fe−AOM) has the potential to act as a CH_4 removal mechanism in SO_4^{2-}-poor systems. Laboratory incubation studies have indeed shown that AOM can be stimulated by Fe-oxide additions.[15,17−19] However, conclusive field evidence for Fe−AOM

Received: July 29, 2014
Revised: November 18, 2014
Accepted: November 20, 2014
Published: November 20, 2014

in brackish surface sediments and knowledge about its significance for global CH_4 dynamics are still lacking.

A basic prerequisite for Fe-mediated AOM is the concurrent presence of porewater CH_4 and abundant reducible Fe-oxides. However, in most brackish and marine sediments the presence of porewater SO_4^{2-} will stimulate microbial SO_4^{2-} reduction and generate dissolved sulfide. This typically results in the reductive dissolution of sedimentary Fe-oxides and the conversion of most reducible Fe to authigenic Fe-sulfides. Significant amounts of Fe-oxides below the zone of SO_4^{2-} reduction in brackish and marine sediments, therefore, are likely mainly found in systems where the input of Fe-oxides is high or where the sediments are subject to transient diagenesis. Examples of the latter are found in the Black Sea[20] and Baltic Sea,[21] where the transition from a freshwater lake to a marine system has led to the preservation of Fe-oxides below sulfidic sediment layers. Other examples of nonsteady-state depositional marine systems where conditions are likely favorable for Fe−AOM include the continental margin off Argentina[22,23] and the Zambezi deep-sea fan sediments[24] where turbidites and other mass flows contribute to rapid burial of reactive Fe (see ref 23 for further examples of marine subsurface sediments with potentially Fe−AOM facilitating conditions). Burial of Fe-oxides below the zone of SO_4^{2-} reduction is also enhanced when Fe-oxides are relatively resistant to reduction, e.g. because of their crystalline nature or changes in surface structure due to adsorption of ions.[25,26] An additional, but still poorly investigated, trigger for transient diagenesis is anthropogenic fertilization of coastal environments.

Here, we provide strong geochemical evidence for Fe-dependent CH_4 oxidation below a shallow sulfate/methane transition zone (SMTZ) in brackish coastal sediments from the Bothnian Sea (salinity 5−6; Figure 1). Furthermore, we show

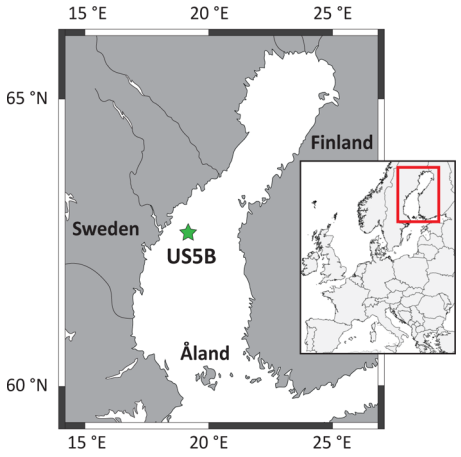

Figure 1. Location map of the study area. Site US5B (62°35.17′ N, 19°58.13′ E) is located in the deepest part of the Bothnian Sea at 214 m depth with an average bottom water salinity of around 6.

that anthropogenic eutrophication may induce nonsteady-state diagenesis, favoring a coupling between Fe-oxide reduction and CH_4 oxidation in coastal sediments. Besides acting as a CH_4 sink, Fe−AOM greatly impacts the biogeochemical cycling of Fe and thereby other tightly coupled element cycles in marine and brackish environments.

MATERIALS AND METHODS

Sediment and Porewater Sampling. Sediment cores (~0−60 cm) were collected from site US5B (62°35.17′ N, 19°58.13′ E) using a GEMAX corer (core diameter 10 cm) during a cruise with R/V *Aranda* in August 2012. All cores were sliced under nitrogen at 1−4 cm resolution. For each slice a subsample was placed in a preweighed glass vial for solid-phase analysis and stored anoxically at −20 °C. Porewater was extracted by centrifugation, filtered through 0.45-μm pore size disposable filters, and subsampled under nitrogen for analysis of dissolved Fe, SO_4^{2-}, and sulfide ($\sum H_2S = H_2S + HS^- + S^{2-}$). Subsamples for total dissolved Fe, which we assume to be present as Fe^{2+}, were acidified with 10 μL of 35% suprapur HCl per ml of subsample and stored at 4 °C until analysis by ICP-OES (PerkinElmer Optima 3000 inductively coupled plasma−optical emission spectroscopy). Porewater SO_4^{2-} was analyzed with ion chromatography (IC) (detection limit of <75 μmol/L) and compared well with total sulfur (S) measured by ICP-OES. Another subsample of 0.5 mL was immediately transferred into glass vials (4 mL) containing 2 mL of 2% zinc (Zn)-acetate solution to precipitate ZnS, and was stored at 4 °C. Sulfide concentrations were then determined spectrophotometrically by complexion of the ZnS precipitate in an acidified solution of phenylenediamine and ferric chloride[27] (detection limit of <1 μmol/L). The sulfide standard was validated by titration with thiosulfate to achieve improved accuracy.

CH_4 samples were taken from a predrilled core directly upon core retrieval. Precisely 10 mL of wet sediment was extracted from each hole and immediately transferred into a 65-mL glass bottle filled with saturated NaCl solution, sealed with a rubber stopper and a screw cap, and subsequently stored upside-down. A headspace of 10 mL of nitrogen was injected and CH_4 concentrations in the headspace were determined by injection of a subsample into a Thermo Finnigan Trace GC gas chromatograph (flame ionization detector). δ^{13}C-CH_4 and δD-CH_4 (D, deuterium) were analyzed by a continuous flow isotope ratio mass spectrometry (CF-IRMS) system at the Institute for Marine and Atmospheric Research Utrecht (IMAU). The amount of CH_4 per sample was often larger than the calibrated range of the isotope ratio mass spectrometer. Therefore, very small amounts of sample were injected via a low-pressure inlet and diluted in helium (He BIP 5.7, Air Products) in a 40-mL sample loop to reach CH_4 mixing ratios of about 2000 ppb. After dilution, the samples were measured as previously described in detail.[28,29]

Sediment samples were freeze-dried, powdered, and ground in an agate mortar inside an argon-filled glovebox. Sediment porosity was determined from the weight loss upon freeze-drying. A split of about 125 mg of freeze-dried sediment was dissolved in a mixture of 2.5 mL of HF (40%) and 2.5 mL of $HClO_4/HNO_3$, in a closed Teflon bomb at 90 °C during one night. The acids were then evaporated at 160 °C and the resulting gel was subsequently dissolved in 1 M HNO_3 at 90 °C during another night. Finally, total elemental concentrations were determined by ICP-OES (precision and accuracy <5%, based on calibration to standard solutions and checked against internal laboratory standard sediments). To correct for variations in terrigenous input of nonreactive Fe, total Fe concentrations were normalized to aluminum (Al), with the input of the latter element assumed to be exclusively from terrestrial sources. To investigate the solid-phase partitioning of Fe, a second 50-mg aliquot of dried sediment was subjected to a sequential extraction procedure for Fe after Poulton and Canfield.[30] Sediment Fe was fractionated into (I) carbonate-associated Fe (including siderite and ankerite, extracted by 1 M Na-acetate brought to pH 4.5 with acetic acid, 24 h), (II) easily reducible (amorphous) oxides

dx.doi.org/10.1021/es503663z | *Environ. Sci. Technol.* 2015, 49, 277−283

($Fe(ox_1)$, including ferrihydrite and lepidocrocite, extracted by 1 M hydroxylamine-HCl, 48 h), (III) reducible (crystalline) oxides ($Fe(ox_2)$, including goethite, hematite, and akagenéite, extracted by Na-dithionite buffer, pH 4.8, 2 h), and (IV) Fe in recalcitrant oxides (mostly magnetite, extracted by 0.2 M ammonium oxalate/0.17 M oxalic acid solution, 2 h). Replicate analyses had a relative error of <5%. A third 0.5-g aliquot of dried sediment was used to determine the amount of FeS_2 (chromium reducible sulfur, CRS, using acidic chromous chloride solution) and FeS (acid volatile sulfur, AVS, using 6 M HCl) via the diffusion-based approach described by Burton et al.[31] and analyzed by iodometric titration of the alkaline Zn acetate trap. Replicate sample extractions yielded reproducibility within 8% for CRS and 10% for AVS. Results for the $Fe(ox_1)$ fraction suggest that most of the AVS present in the SMTZ was extracted during the hydroxylamine-HCl step (Supporting Information (SI) Figure S1). Thus, the estimation of the reducible sedimentary Fe-oxide content ($Fe(ox_1)$ + $Fe(ox_2)$) shown in Figure 2 was corrected for AVS dissolution within the SMTZ.

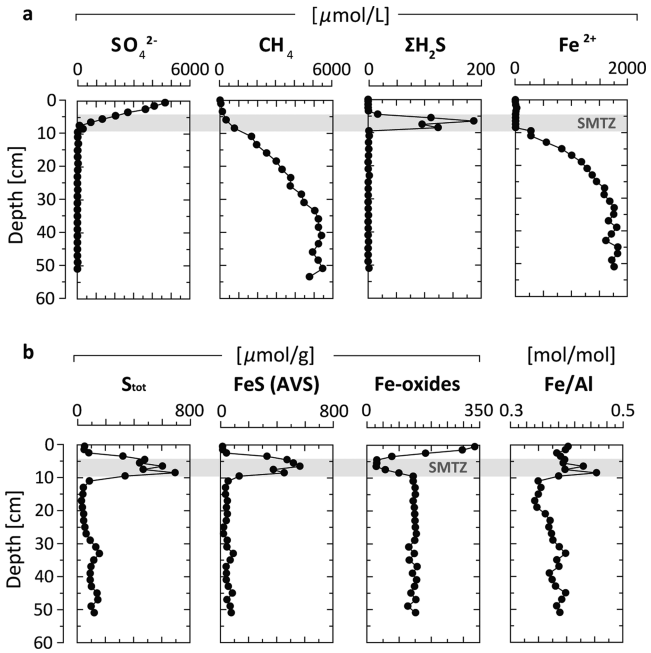

Figure 2. Geochemical profiles for site US5B. (a) Porewater profiles of SO_4^{2-}, CH_4, sulfide ($\sum H_2S = H_2S + HS^- + S^{2-}$), and Fe^{2+}. Gray bar indicates the sulfate/methane transition zone (SMTZ). (b) Sediment profiles of total sulfur (S_{tot}), FeS (acid volatile sulfide, AVS), Fe-oxides (see SI Figure S1 for the calculation of the Fe-oxide fraction), and total (Fe/Al).

Incubation Experiments. Replicate sediment cores taken in 2012 were sealed immediately and stored onboard at 4 °C. Back in the lab, they were sliced in sections of 5 cm under strictly anaerobic conditions and stored anaerobically in the dark at 4 °C. The incubation experiments started within half a year after sampling. Per culture bottle, 30 g of wet sediment (~25 mL) was homogenized in 75 mL of SO_4^{2-}-depleted medium mimicking in situ bottom water conditions within a helium-filled glovebox (containing ~2% hydrogen gas, H_2). An 85-mL aliquot of this sediment/medium slurry was distributed over 150-mL culture bottles and an additional 11.4 mL of medium was added to all bottles with the exception of the Fe treatments, for which 11.4 mL of a Fe-nanoparticle solution[32] (20 mmol/L ferric Fe (Fe(III)), resulting in 2 mmol Fe(III) per bottle) was added instead. The approximate ratio of 1 part sediment to 3 parts medium was chosen in agreement to reported incubation studies.[15,18] After the contents were mixed, the culture bottles were sealed with airtight red butyl rubber stoppers and secured with open-top Al screw caps. After being sealed, 5 mL of CO_2 and either 45 mL of nitrogen ("cntl") or 45 mL of $^{13}CH_4$ ("$^{13}CH_4$" and "$^{13}CH_4$ & Fe(III)") were injected into the headspace of duplicate incubations to yield 1 bar overpressure (volume headspace = 50 mL) and incubated in the dark at 20 °C under gentle shaking. Dissolved sulfide and SO_4^{2-} were sampled within the glovebox by allowing the sediment to settle out of suspension and taking a subsample (1.5 mL) of the supernatant water via a needle syringe. Analysis of sulfide was performed as described above for sediment porewater (detection limit of <1 μmol/L). Samples for total dissolved S were measured by ICP-OES after acidification with 10 μL of 35% suprapur HCl and assumed to represent only SO_4^{2-} due to the release of sulfide to the gas phase during acidification[33] (detection limit of <82 μmol/L). Headspace samples (30 μL) were analyzed by gas chromatography (GC, Agilent 6890 series, USA) using a Porapak Q column at 80 °C (5 min) with helium as the carrier gas (flow rate 24 mL/min). The GC was coupled to a mass spectrometer (Agilent 5975C inert MSD, Agilent, USA) to quantify the masses 44 and 45 (CO_2). To account for the medium loss due to subsampling of the solution and because of an observed leveling-off of measured headspace $^{13}CO_2$ concentrations, an additional 11.4 mL of medium ("cntl" and "$^{13}CH_4$") and Fe-nanoparticle solution ("$^{13}CH_4$ & Fe(III)") was added to the culture bottles after 55 days (indicated by a dashed line in Figure 3 and SI Figure S2). Fe–AOM rates were determined from the linear slope of $^{13}CO_2$ production in duplicate incubations from 20–30 cm and 30–35 cm depths, before and after second addition of Fe(III) (SI Figure

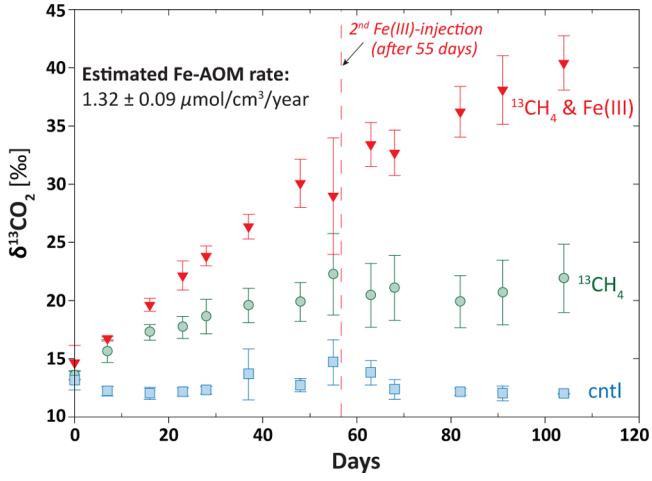

Figure 3. Incubation experiment with ^{13}C-labeled CH_4 conducted on sediments from 20–35 cm depth. SO_4^{2-}-depleted slurry incubations showed an increasing enrichment of headspace CO_2 in ^{13}C after addition of Fe(III) ("$^{13}CH_4$ & Fe(III)", red triangles) compared to treatments where no additional Fe(III) was added ("$^{13}CH_4$", green circles), suggesting stimulation of Fe–AOM. Elevated $\delta^{13}C–CO_2$ values ($[^{13}CO_2]/([^{12}CO_2]+[^{13}CO_2])$) of the $^{13}CH_4$-treatment without additional Fe(III) compared to the control ("cntl", blue squares) indicate Fe–AOM with remaining Fe-oxides present in the sediment. Twenty mmol/L Fe(III) was added at t_0 (0 days) and after 55 days (dashed red line). Error bars are based on duplicates for 20–30 cm and 30–35 cm (i.e., n = 4; see SI Figure S2 for the calculation of the Fe–AOM rate).

dx.doi.org/10.1021/es503663z | Environ. Sci. Technol. 2015, 49, 277–283

S2), taking into account the CO_2 dissolved in the liquid and removal thereof during sampling. Thus, the statistical mean is based on a total number of eight rate estimates.

Diffusion Model Simulations. A column diffusion model was used to test different hypotheses for sources and sinks of CH_4 within the sediment at station US5B. The model represents the sediment column from the surface to a depth of 36 cm, using 72 layers of 0.5 cm each. Concentrations of total CH_4, δD-CH_4, and δ^{13}C-CH_4 are simulated, accounting for production, loss and diffusion, and their corresponding isotopic fractionation. The model was run to steady state for each scenario. As the boundary condition at 36 cm depth we constrain the model with the measured values of CH_4, δD-CH_4 and δ^{13}C-CH_4. At the surface, the flux to the water column was set to zero. The diffusion coefficient for CH_4 was corrected for in situ temperature, salinity, and porosity (see Supporting Information). A diffusion fractionation of $\varepsilon_{Diffusion}$ = 3 ‰ for both ^{13}C-CH_4 and D-CH_4 was assumed according to refs 34 and 35.

Two zones were defined within the sediment column, 0−8.5 cm and 8.5−36 cm, with constant production and loss parameters within each zone. The first zone represents SO_4−AOM, while the second represents the area where both CH_4 loss through Fe−AOM and CH_4 production through methanogenesis may occur. We performed three model simulations: "with Fe−AOM", "no Fe−AOM", and "diffusion only". The rate constants and fractionation factors used in these simulations for the CH_4 production and removal processes are presented in SI Table S3.

RESULTS AND DISCUSSION

Geochemical Profiles. Vertical porewater profiles for station US5B (Figure 2) reveal a shallow SMTZ at a depth of ca. 4−8.5 cm, where SO_4^{2-}-dependent AOM results in the depletion of porewater SO_4^{2-} and CH_4. Dissolved SO_4^{2-} decreases from 4.9 mmol/L at the sediment water interface to 0.3 mmol/L at the bottom of the SMTZ, and stayed below the detection limit of 75 μmol/L throughout the rest of the core. Reductive dissolution of Fe-oxides driven by sulfide production during SO_4−AOM induces a distinct minimum in sedimentary Fe-oxides and precipitation of Fe-sulfides (mostly FeS). Abundant reducible Fe-oxides below the SMTZ are accompanied by very high dissolved ferrous Fe (Fe^{2+}) concentrations (>1.8 mmol/L). The depth trend in total (Fe/Al) indicates that the Fe is not only repartitioned between oxide and sulfide phases within the SMTZ, but that Fe-oxide reduction below the SMTZ triggers upward migration of dissolved Fe^{2+} with an enrichment of total Fe in the sulfidic zone. However, in contrast to the SMTZs observed at greater depth (>1.5 m) in sediments of the Baltic Sea[21] and Black Sea,[20] sulfide generated by SO_4^{2-} reduction is all sequestered in the form of authigenic Fe-sulfides in the shallow SMTZ observed in this study (Figure 2). Thus, no sulfide remains to diffuse downward into the zone where Fe reduction is occurring. Reductive Fe-oxide dissolution by dissolved sulfide in the deeper sediments is therefore not possible. Although a cryptic sulfur cycle where SO_4^{2-} is generated by sulfide reacting with deeply buried Fe(III) species[20,21] is unlikely to occur, ^{35}S radiotracer measurements of SO_4^{2-} reduction rates would be needed to completely exclude the possibility of a cryptic sulfur cycle through reoxidation of Fe sulfide minerals. High dissolved Fe^{2+} concentrations further preclude Fe-oxide reduction via sulfide released during disproportionation of elemental sulfur,[36,37] as any sulfide produced locally would be immediately scavenged to form Fe-sulfides. Thus, there are only two alternative mechanisms that may explain the high dissolved Fe^{2+} concentration in the porewater below the SMTZ. The first mechanism is organoclastic Fe reduction, i.e. Fe reduction coupled to organic matter degradation. The second is Fe−AOM, i.e. Fe reduction coupled to AOM. In the following, we demonstrate why the latter mechanism is the process most likely responsible for the high dissolved Fe^{2+} in these sediments.

Fe−AOM Activity below the SMTZ. The potential of the microbial community present in the sediments below the SMTZ to perform Fe−AOM was experimentally tested with slurry incubation studies. Fresh sediment samples from several depth layers were incubated with ^{13}C-labeled CH_4 ($^{13}CH_4$), CO_2, and a SO_4^{2-}-depleted medium mimicking Bothnian Sea bottom water conditions. Duplicate incubations were amended with either only $^{13}CH_4$ or $^{13}CH_4$ and 20 mmol/L Fe hydroxide nanoparticles.[32] In the control slurries, nitrogen was used instead of $^{13}CH_4$. AOM rates were then determined by measuring production of $^{13}CO_2$, i.e. the end product of $^{13}CH_4$ oxidation. The addition of Fe hydroxide nanoparticles almost doubled AOM activity (1.7 fold increase) in the sediment samples between 20 and 35 cm depth compared to the slurries where no additional Fe(III) was added (Figure 3). The increase in δ^{13}C−CO_2 as a response to Fe(III) addition thus suggests that the microbial community present in the sediment below the SMTZ is capable of coupling AOM to Fe reduction. Throughout the whole experiment, sulfide stayed below detection limit (<1 μmol/L) and SO_4^{2-} concentrations stayed below 350 μmol/L. A slight decrease in background SO_4^{2-} during the incubation period might indicate low levels of SO_4^{2-} reduction of ∼1.9 pmol SO_4^{2-} cm^{-3} day^{-1}. Similar rates of SO_4^{2-} reduction (∼1 pmol SO_4^{2-} cm^{-3} day^{-1}) were reported for methanogenic Baltic Sea sediments.[21] Taking into account indirect Fe stimulated SO_4^{2-}-driven AOM[19] through a cryptic sulfur cycle,[20,21] where redox reactions between sulfide and Fe-oxides result in the reoxidation of sulfide to SO_4^{2-} in a 17:1 stoichiometric ratio, we estimate a gross rate of SO_4^{2-} reduction of ∼2 pmol SO_4^{2-} cm^{-3} day^{-1}. SO_4−AOM is thus unlikely to contribute more than 0.1% to the total $^{13}CO_2$ production observed in our incubations. These findings support our hypothesis that the accumulation of dissolved Fe^{2+} in the porewater below the SMTZ is, at least partly, a result of Fe−AOM. The potential rate of Fe−AOM in our incubations is 1.32 ± 0.09 μmol cm^{-3} year^{-1} (see SI Figure S2), which compares well to recent estimates of potential Fe−AOM rates in slurry incubations of brackish wetland (1.42 ± 0.11 μmol cm^{-3} year^{-1};[15]) and Fe(III)-amended mesocosm studies of intact deep lake sediment cores (1.26 ± 0.63 μmol cm^{-3} year^{-1};[13]). It should be noted, however, that these rates all derive from stimulated microbial communities and thus could be lower under in situ conditions.

Isotopic Evidence for Concurrent Methanogenesis. Porewater profiles of δD-CH_4 and δ^{13}C-CH_4 (Figure 4a) show the common features observed in marine sediments where methanogenesis deep in the sediment results in the buildup of isotopically depleted CH_4 in the porewater.[38] The preferential oxidation of isotopically light CH_4 during AOM[39,40] results in a progressive enrichment of the residual CH_4 in ^{13}C-CH_4 and D-CH_4 toward the sediment surface. Application of the Rayleigh distillation function[12,38,41] reveals two distinct sets of kinetic isotope fractionation factors for hydrogen (ε_H) and carbon (ε_C) that are spatially separated (Figure 4b). The sympathetic change in the ^{13}C and D content from 4−8.5 cm depth is driven by SO_4−AOM within the SMTZ. Corresponding isotope fractionations

dx.doi.org/10.1021/es503663z | Environ. Sci. Technol. 2015, 49, 277−283

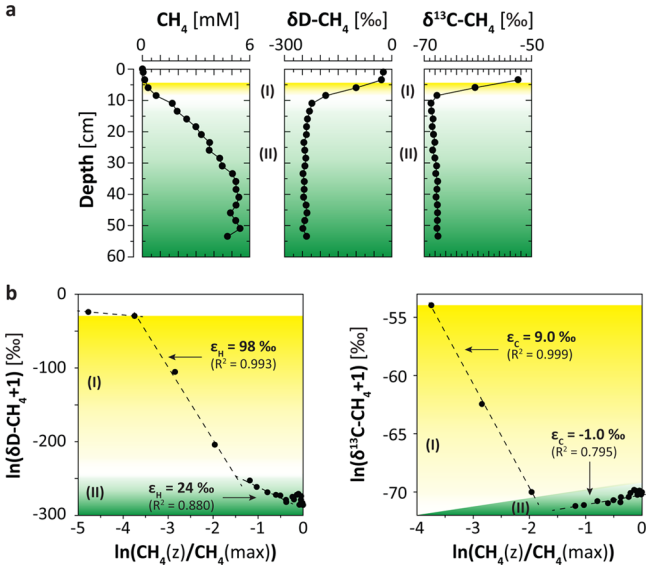

Figure 4. Isotopic composition of porewater methane. (a) Vertical porewater profiles for total CH_4, δD-CH_4 (in ‰ vs Standard Mean Ocean Water; SMOW) and δ^{13}C-CH_4 (in ‰ vs Vienna Pee Dee Belemnite; VPDB). (b) Rayleigh fractionation plots for δD-CH_4 (left) and δ^{13}C-CH_4 (right). The yellow area (I) indicates the depth zone of SO_4–AOM, i.e. the SMTZ, while the green area (II) shows all measurements below the SMTZ. Different slopes between I (yellow) and II (green) reveal two distinct kinetic isotope fractionation factors for hydrogen (ε_H) and carbon (ε_C) that are spatially separated. SO_4–AOM drives a sympathetic change in C and D isotopes (area I), whereas the antipathetic change in area II indicates hydrogenotrophic CH_4 production.

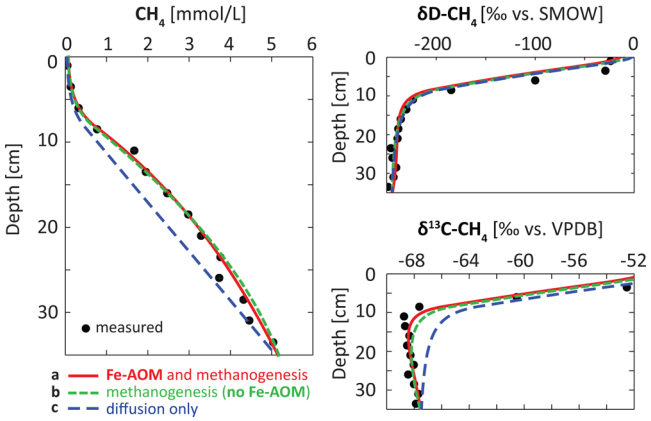

Figure 5. Column diffusion model simulations of the total concentration and isotopic composition of porewater CH_4 at station US5B. SO_4–AOM (between 0 and 8.5 cm) is represented in all model simulations (a–c), whereas different scenarios for the fate of CH_4 below the SMTZ (8.5–36 cm) were tested. (a) CH_4 loss through Fe–AOM and concurrent CH_4 production through methanogenesis; (b) only CH_4 production but no removal through Fe–AOM; (c) upward diffusing CH_4 with no further alteration. SMOW = Standard mean ocean water and VPDB = Vienna Pee Dee Belemnite. See SI Table S3 for details about rate constants and fractionation factors used in the model simulations.

($\varepsilon_H = 98 \pm 0.3$ ‰, $\varepsilon_C = 9 \pm 0.2$ ‰, see Figure 4b) are at the low end of reported values from near coastal sediments in the Baltic Sea (ε_H = 100–140 ‰, ε_C = 11–13 ‰)[40] and SO_4–AOM in general.[38,39,42] The isotopic composition of CH_4 below the SMTZ, on the other hand, shows enrichment in D isotopes but depletion in ^{13}C ($\varepsilon_H = 24 \pm 0.1$ ‰, $\varepsilon_C = -1 \pm 0.04$ ‰, see Figure 4b). Such antipathetic changes are usually attributed to CH_4 production,[38,43] with hydrogenotrophic methanogenesis (CO_2 reduction by H_2) as the most likely methanogenic pathway for the range of CH_4 isotope ratios observed at station US5B.[38]

Fe–AOM as the main contributor to Fe^{2+} production and CH_4 removal would be expected to isotopically enrich porewater CH_4 in both heavy isotopes below the SMTZ, in contrast to the observations. We hypothesized that production of isotopically light CH_4 during methanogenesis counteracts the progressive enrichment of isotopically heavy CH_4 during Fe–AOM. Indeed, simulations of the isotopic composition of porewater CH_4 at station US5B using a column diffusion model could successfully reproduce the observed patterns in δD-CH_4 and δ^{13}C-CH_4 when assuming the concurrent presence of Fe–AOM and hydrogenotrophic methanogenesis (Figure 5). Because of the slow rate of CH_4 oxidation, Fe–AOM only removes a small amount of porewater CH_4. Hence, modeled profiles of δD-CH_4 and δ^{13}C-CH_4 are highly sensitive to the rate of methanogenesis and the assumed values of ε_H and ε_C, which have a wide reported range.[38] Our simulations show that the measurements can also be approximated without Fe–AOM, when altered CH_4 production rates and methanogenic fractionation factors are used in the model. Nevertheless, the model does demonstrate that methanogenesis is required to reproduce the porewater concentration and isotope profiles of CH_4; removal in the SMTZ only and diffusion from depth cannot explain the observed trends. This provides conclusive evidence for methanogenesis within the zone of Fe reduction.

However, hydrogenotrophic Fe-reducers coupling H_2 oxidation to Fe(III) reduction are known to be able to outcompete methanogens for H_2 by maintaining the H_2 concentrations at levels that are too low for methanogens to grow.[44–46] In addition, direct inhibition of methanogenesis by Fe(III) has been reported.[47–49] The high demand for H_2 needed to explain the dissolved Fe^{2+} concentrations (2:1 stoichiometry)[44,50] could therefore result in a competitive inhibition of hydrogenotrophic methanogenesis. Here we clearly demonstrate the co-occurrence of Fe reduction and methanogenesis, indicating that reduction of Fe(III) by H_2 is unlikely to be the main reason for the high dissolved Fe^{2+} below the SMTZ. Consequently, we conclude that CH_4 might be a plausible electron donor for the reduction of relatively refractory Fe-oxides under methanogenic conditions. Our field data and model results further imply that the imprint of Fe–AOM on the isotopic composition of porewater CH_4 may be masked when co-occurring with methanogenesis.

Fe–AOM and Coastal Eutrophication. In the Bothnian Sea, the shallow position of the SMTZ is linked to anthropogenic eutrophication over recent decades. Long-term monitoring studies based on water transparency, inorganic nutrients, and chlorophyll a in the Bothnian Sea[51,52] indicate that, throughout the last century, anthropogenic loading of nutrients derived from land has enhanced primary productivity and subsequent export production of organic matter. As a consequence, rates of SO_4^{2-} reduction and methanogenesis likely increased, initiating an upward migration of the SMTZ. Since the early 2000s, eutrophication of the Bothnian Sea has started to decline again,[51,52] halting the upward movement of the SMTZ at its current position. Evidence for a rapid upward shift of the SMTZ and its recent fixation is provided by the distinct enrichment of authigenic Fe-sulfides around the present day SMTZ.[16,22,24,53,54] The diffusive influx of SO_4^{2-} into the SMTZ (~1 mol m^{-2} $year^{-1}$; Figure 2) and the S content of the Fe-sulfide enrichment (~10

dx.doi.org/10.1021/es503663z | Environ. Sci. Technol. 2015, 49, 277–283

mol m^{-2}; Figure 2) suggest that the fixation of the SMTZ in its current position occurred approximately 10 years before the time of sampling, consistent with earlier findings at site US5B.[16] This rapid upward displacement of the SMTZ in response to eutrophication likely reduced the exposure time of sedimentary Fe-oxides to dissolved sulfide, allowing a portion of Fe-oxides to remain preserved below the newly established SMTZ and facilitating Fe−AOM. Because many coastal environments have experienced eutrophication in recent decades,[55] we postulate that such transient diagenesis may be widespread, creating similar zones of Fe−AOM in Fe-oxide rich brackish coastal sediments worldwide.

Biogeochemical Implications. Although Fe-oxides are abundant in the sediments below the SMTZ, their bioavailability may be limiting Fe-dependent AOM. This is implied by the coexistence of both CH_4 and Fe-oxides in the same zone and the clear stimulation of CH_4 oxidation after addition of Fe nanoparticles. Our incubation and modeling results suggest that Fe−AOM accounts for ∼3% of total CH_4 removal in Bothnian Sea sediments (see Supporting Information for calculations), contributing strongly to Fe^{2+} production due to the 8:1 Fe−CH_4 stoichiometry (eq 2). The remaining CH_4 is likely removed by SO_4−AOM and aerobic CH_4 oxidation at the sediment surface. The large amount of reactive Fe-oxides needed to oxidize significant amounts of CH_4 and the low measured reaction rates (Figure 3) imply that Fe−AOM probably does not contribute more than a few percent to CH_4 oxidation in modern marine and brackish surface sediments. However, Fe−AOM could significantly impact the biogeochemical cycles of other elements. For example, high porewater Fe^{2+} may be especially conducive to in situ formation of ferrous-phosphate minerals, thus increasing the sequestration of phosphorus in the sediment and providing a negative feedback on coastal eutrophication.[16] By inducing nonsteady-state diagenesis in aquatic sediments, future climate change and eutrophication may increase the global importance of Fe−AOM and its impact on other biogeochemical cycles.

■ ASSOCIATED CONTENT

Supporting Information

Description of porewater calculations and model details, correction of AVS dissolution during Fe-oxide extraction (Figure S1), determination of Fe−AOM rate (Figure S2), measured porewater (Table S1) and solid-phase concentrations (Table S2), and model parameters used for the different simulations (Table S3). This material is available free of charge via the Internet at http://pubs.acs.org/.

■ AUTHOR INFORMATION

Corresponding Author

*Phone: +31 30 253 3264; e-mail: m.j.egger@uu.nl.

Present Address

⊥Now at Department of Environmental Sciences, University of Helsinki, Viikinkaari 2a, 00014 Helsinki, Finland.

Author Contributions

C.P.S. conceived and designed the field study. M.E. and T.J. carried out the fieldwork. M.E., C.P.S., O.R., K.F.E., B.K., and M.S.M.J. designed incubation experiments. M.E., O.R., and K.F.E. performed and analyzed experiments. C.J.S., C.v.d.V., and T.R. performed methane isotope analysis. M.E. analyzed fieldwork samples and compiled all data. N.B. designed the diffusion model applied for methane isotopes. M.E. and C.P.S. wrote the manuscript with contributions of all coauthors.

Notes

The authors declare no competing financial interest.

■ ACKNOWLEDGMENTS

We thank the captain, crew, and scientific participants aboard R/V *Aranda* in 2012 and P. Kotilainen for their assistance with the fieldwork, and D. van de Meent, H. de Waard, and T. Zalm for analytical assistance in Utrecht. This work was funded by ERC Starting Grant 278364 (to C.P.S.). O.R. was supported by ERC Advanced Grant 2322937. M.S.M.J. was supported by ERC Advanced Grant 339880 and OCW/NWO Gravitation Grant SIAM 024002002. K.F.E. was supported by the Darwin Center for Biogeology (project 3071) and VENI grant 863.13.007 from the Dutch Science Foundation (NWO). B.K. was supported by VENI grant 863.11.003 from NWO.

■ REFERENCES

(1) Myhre, G.; Schindell, D.; Bréon, F. M.; Collins, W.; Fuglestvedt, J.; Huang, J.; Koch, D.; Lamarque, J. F.; Lee, D.; Mendoza, B.; et al. Anthropogenic and natural radiative forcing. In *Climate Change 2013: The Physical Science Basis*; Stocker, T. F., Qin, D., Plattner, G. K., Tignor, M., Allen, S. K., Boschung, J., Nauels, A., Xia, Y., Bex, V., Midgley, P. M., Eds.; Cambridge University Press: Cambridge, U. K. and New York, 2013.

(2) Reeburgh, W. S. Oceanic methane biogeochemistry. *Chem. Rev.* **2007**, *107*, 486−513.

(3) Knittel, K.; Boetius, A. Anaerobic oxidation of methane: Progress with an unknown process. *Annu. Rev. Microbiol.* **2009**, *63*, 311−334.

(4) Barnes, R. O.; Goldberg, E. D. Methane production and consumption in anoxic marine sediments. *Geology* **1976**, *4*, 297−300.

(5) Reeburgh, W. S. Methane consumption in Cariaco Trench waters and sediments. *Earth Planet. Sci. Lett.* **1976**, *28*, 337−344.

(6) Martens, C. S.; Berner, R. A.; Rosenfeld, J. K. Interstitial water chemistry of anoxic Long Island Sound sediments. 2. Nutrient regeneration and phosphate removal. *Limnol. Oceanogr.* **1978**, *23*, 605−617.

(7) Iversen, N.; Jørgensen, B. B. Anaerobic methane oxidation rates at the sulfate-methane transition in marine sediments from Kattegat and Skagerrak (Denmark). *Limnol. Oceanogr.* **1985**, *30*, 944−955.

(8) Hoehler, T. M.; Alperin, M. J.; Albert, D. B.; Martens, C. S. Field and laboratory studies of methane oxidation in an anoxic marine sediment: Evidence for a methanogen-sulfate reducer consortium. *Global Biogeochem. Cycles* **1994**, *8*, 451−463.

(9) Boetius, A.; Ravenschlag, K.; Schubert, C. J.; Rickert, D.; Widdel, F.; Gieseke, A.; Amann, R.; Jørgensen, B. B.; Witte, U.; Pfannkuche, O. A marine microbial consortium apparently mediating anaerobic oxidation of methane. *Nature* **2000**, *407*, 623−626.

(10) Milucka, J.; Ferdelman, T. G.; Polerecky, L.; Franzke, D.; Wegener, G.; Schmid, M.; Lieberwirth, I.; Wagner, M.; Widdel, F.; Kuypers, M. M. M. Zero-valent sulphur is a key intermediate in marine methane oxidation. *Nature* **2012**, *491*, 541−546.

(11) Wersin, P.; Hoehener, P.; Giovanoli, R.; Stumm, W. Early diagenetic influences on iron transformations in a freshwater lake sediment. *Chem. Geol.* **1991**, *90*, 233−252.

(12) Crowe, S. A.; Katsev, S.; Leslie, K.; Sturm, A.; Magen, C.; Nomosatryo, S.; Pack, M. A.; Kessler, J. D.; Reeburgh, W. S.; Roberts, J. A.; et al. The methane cycle in ferruginous Lake Matano. *Geobiology* **2011**, *9*, 61−78.

(13) Sivan, O.; Adler, M.; Pearson, A.; Gelman, F.; Bar-Or, I.; John, S. G.; Eckert, W. Geochemical evidence for iron-mediated anaerobic oxidation of methane. *Limnol. Oceanogr.* **2011**, *56*, 1536−1544.

(14) Nordi, K. Á.; Thamdrup, B.; Schubert, C. J. Anaerobic oxidation of methane in an iron-rich Danish freshwater lake sediment. *Limnol. Oceanogr.* **2013**, *58*, 546−554.

(15) Segarra, K. E. A.; Comerford, C.; Slaughter, J.; Joye, S. B. Impact of electron acceptor availability on the anaerobic oxidation of methane in coastal freshwater and brackish wetland sediments. *Geochim. Cosmochim. Acta* **2013**, *115*, 15−30.
(16) Slomp, C. P.; Mort, H. P.; Jilbert, T.; Reed, D. C.; Gustafsson, B. G.; Wolthers, M. Coupled dynamics of iron and phosphorus in sediments of an oligotrophic coastal basin and the impact of anaerobic oxidation of methane. *PLoS One* **2013**, *8*, e62386.
(17) Adler, M.; Eckert, W.; Sivan, O. Quantifying rates of methanogenesis and methanotrophy in Lake Kinneret sediments (Israel) using pore-water profiles. *Limnol. Oceanogr.* **2011**, *56*, 1525−1535.
(18) Beal, E. J.; House, C. H.; Orphan, V. J. Manganese- and iron-dependent marine methane oxidation. *Science* **2009**, *325*, 184−187.
(19) Sivan, O.; Antler, G.; Turchyn, A. V.; Marlow, J. J.; Orphan, V. J. Iron oxides stimulate sulfate-driven anaerobic methane oxidation in seeps. *Proc. Natl. Acad. Sci. U. S. A.* **2014**, 1−9.
(20) Holmkvist, L.; Kamyshny, A.; Vogt, C.; Vamvakopoulos, K.; Ferdelman, T. G.; Jørgensen, B. B. Sulfate reduction below the sulfate−methane transition in Black Sea sediments. *Deep Sea Res., Part I* **2011**, *58*, 493−504.
(21) Holmkvist, L.; Ferdelman, T. G.; Jørgensen, B. B. A cryptic sulfur cycle driven by iron in the methane zone of marine sediment (Aarhus Bay, Denmark). *Geochim. Cosmochim. Acta* **2011**, *75*, 3581−3599.
(22) Riedinger, N.; Pfeifer, K.; Kasten, S.; Garming, J. F. L.; Vogt, C.; Hensen, C. Diagenetic alteration of magnetic signals by anaerobic oxidation of methane related to a change in sedimentation rate. *Geochim. Cosmochim. Acta* **2005**, *69*, 4117−4126.
(23) Riedinger, N.; Formolo, M. J.; Lyons, T. W.; Henkel, S.; Beck, A.; Kasten, S. An inorganic geochemical argument for coupled anaerobic oxidation of methane and iron reduction in marine sediments. *Geobiology* **2014**, *12*, 172−181.
(24) März, C.; Hoffmann, J.; Bleil, U.; de Lange, G. J.; Kasten, S. Diagenetic changes of magnetic and geochemical signals by anaerobic methane oxidation in sediments of the Zambezi deep-sea fan (SW Indian Ocean). *Mar. Geol.* **2008**, *255*, 118−130.
(25) Lovley, D. R.; Phillips, E. J. P. Availability of ferric iron for microbial reduction in bottom sediments of the freshwater tidal Potomac River. *Appl. Environ. Microbiol.* **1986**, *52*, 751−757.
(26) Roden, E. E. Diversion of electron flow from methanogenesis to crystalline Fe(III) oxide reduction in carbon-limited cultures of wetland sediment microorganisms. *Appl. Environ. Microbiol.* **2003**, *69*, 5702−5706.
(27) Cline, J. D. Spectrophotometric determination of hydrogen sulfide in natural waters. *Limnol. Oceanogr.* **1969**, *14*, 454−458.
(28) Brass, M.; Röckmann, T. Continuous-flow isotope ratio mass spectrometry method for carbon and hydrogen isotope measurements on atmospheric methane. *Atmos. Meas. Technol.* **2010**, *3*, 1707−1721.
(29) Sapart, C. J.; van der Veen, C.; Vigano, I.; Brass, M.; van de Wal, R. S. W.; Bock, M.; Fischer, H.; Sowers, T.; Buizert, C.; Sperlich, P.; et al. Simultaneous stable isotope analysis of methane and nitrous oxide on ice core samples. *Atmos. Meas. Technol.* **2011**, *4*, 2607−2618.
(30) Poulton, S.; Canfield, D. Development of a sequential extraction procedure for iron: Implications for iron partitioning in continentally derived particulates. *Chem. Geol.* **2005**, *214*, 209−221.
(31) Burton, E. D.; Sullivan, L. A.; Bush, R. T.; Johnston, S. G.; Keene, A. F. A simple and inexpensive chromium-reducible sulfur method for acid-sulfate soils. *Appl. Geochem.* **2008**, *23*, 2759−2766.
(32) Bosch, J.; Heister, K.; Hofmann, T.; Meckenstock, R. U. Nanosized iron oxide colloids strongly enhance microbial iron reduction. *Appl. Environ. Microbiol.* **2010**, *76*, 184−190.
(33) Jilbert, T.; Slomp, C. P. Iron and manganese shuttles control the formation of authigenic phosphorus minerals in the euxinic basins of the Baltic Sea. *Geochim. Cosmochim. Acta* **2013**, *107*, 155−169.
(34) Happell, J. D.; Chanton, J. P.; Showers, W. J. Methane transfer across the water-air interface in stagnant wooded swamps of Florida: Evaluation of mass-transfer coefficients and isotopic fractionation. *Limnol. Oceanogr.* **1995**, *40*, 290−298.
(35) Chanton, J. P. The effect of gas transport on the isotope signature of methane in wetlands. *Org. Geochem.* **2005**, *36*, 753−768.
(36) Bak, F.; Pfennig, N. Chemolithotrophic growth of *Desulfovibrio sulfodismutans* sp. nov. by disproportionation of inorganic sulfur compounds. *Arch. Microbiol.* **1987**, *147*, 184−189.
(37) Thamdrup, B.; Finster, K.; Hansen, J. W.; Bak, F. Bacterial disproportionation of elemental sulfur coupled to chemical reduction of iron or manganese. *Appl. Environ. Microbiol.* **1993**, *59*, 101−108.
(38) Whiticar, M. J. Carbon and hydrogen isotope systematics of bacterial formation and oxidation of methane. *Chem. Geol.* **1999**, *161*, 291−314.
(39) Alperin, M. J.; Reeburgh, W. S.; Whiticar, M. J. Carbon and hydrogen isotope fractionation resulting from anaerobic methane oxidation. *Global Biogeochem. Cycles* **1988**, *2*, 279−288.
(40) Martens, C. S.; Albert, D. B.; Alperin, M. J. Stable isotope tracing of anaerobic methane oxidation in the gassy sediments of Eckernforde Bay, German Baltic Sea. *Am. J. Sci.* **1999**, *299*, 589−610.
(41) Rayleigh, J. W. S. Theoretical considerations respecting the separation of gases by diffusion and similar processes. *Philos. Mag.* **1896**, *42*, 493−499.
(42) Holler, T.; Wegener, G.; Knittel, K.; Boetius, A.; Brunner, B.; Kuypers, M. M. M.; Widdel, F. Substantial (13) C/(12) C and D/H fractionation during anaerobic oxidation of methane by marine consortia enriched in vitro. *Environ. Microbiol. Rep.* **2009**, *1*, 370−376.
(43) Chanton, J.; Chaser, L.; Glasser, P.; Siegel, D. Carbon and hydrogen isotopic effects in microbial methane from terrestrial environments. In *Stable Isotopes and Biosphere-Atmosphere Interactions*; Flanagan, L., Ed.; Elsevier-Academic Press: Amsterdam, 2005; pp 85−105.
(44) Lovley, D. R.; Phillips, E. J. P.; Lonergan, D. J. Hydrogen and formate oxidation coupled to dissimilatory reduction of iron or manganese by *Alteromonas putrefaciens*. *Appl. Environ. Microbiol.* **1989**, *55*, 700−706.
(45) Achtnich, C.; Bak, F.; Conrad, R. Competition for electron donors among nitrate reducers, ferric iron reducers, sulfate reducers, and methanogens in anoxic paddy soil. *Biol. Fertil. Soils* **1995**, *19*, 65−72.
(46) Reiche, M.; Torburg, G.; Küsel, K. Competition of Fe(III) reduction and methanogenesis in an acidic fen. *FEMS Microbiol. Ecol.* **2008**, *65*, 88−101.
(47) Bond, D. R.; Lovley, D. R. Reduction of Fe(III) oxide by methanogens in the presence and absence of extracellular quinones. *Environ. Microbiol.* **2002**, *4*, 115−124.
(48) Bodegom, P. M.; Scholten, J. C. M.; Stams, A. J. M. Direct inhibition of methanogenesis by ferric iron. *FEMS Microbiol. Ecol.* **2004**, *49*, 261−268.
(49) Liu, D.; Wang, H.; Dong, H.; Qiu, X.; Dong, X.; Cravotta, C. A. Mineral transformations associated with goethite reduction by *Methanosarcina barkeri*. *Chem. Geol.* **2011**, *288*, 53−60.
(50) Thauer, R. K.; Jungermann, K.; Decker, K. Energy conservation in chemotrophic anaerobic bacteria. *Bacteriol. Rev.* **1977**, *41*, 809.
(51) Fleming-Lehtinen, V.; Laamanen, M.; Kuosa, H.; Haahti, H.; Olsonen, R. Long-term development of inorganic nutrients and chlorophyll alpha in the open northern Baltic Sea. *Ambio* **2008**, *37*, 86−92.
(52) Fleming-Lehtinen, V.; Laamanen, M. Long-term changes in secchi depth and the role of phytoplankton in explaining light attenuation in the Baltic Sea. *Estuarine Coastal Shelf Sci.* **2012**, *102*−*103*, 1−10.
(53) Kasten, S.; Freudenthal, T.; Gingele, F. X.; Schulz, H. D. Simultaneous formation of iron-rich layers at different redox boundaries in sediments of the Amazon deep-sea fan. *Geochim. Cosmochim. Acta* **1998**, *62*, 2253−2264.
(54) Hensen, C.; Zabel, M.; Pfeifer, K.; Schwenk, T.; Kasten, S.; Riedinger, N.; Schulz, H.; Boetius, A. Control of sulfate pore-water profiles by sedimentary events and the significance of anaerobic oxidation of methane for the burial of sulfur in marine sediments. *Geochim. Cosmochim. Acta* **2003**, *67*, 2631−2647.
(55) Diaz, R. J.; Rosenberg, R. Spreading dead zones and consequences for marine ecosystems. *Science* **2008**, *321*, 926−929.